Effect of near-earth thunderstorms electric field on the intensity of ground cosmic ray positrons/electrons in Tibet

X.X. Zhou*, X.J. Wang, D.H. Huang, H.Y. Jia

School of Physical Science and Technology, Southwest Jiaotong University, 111, Er Huan Lu Bei Yi Duan, Chengdu 610031, China

ARTICLE INFO

ABSTRACT

Monte Carlo simulations are performed to study the correlation between the ground cosmic ray intensity and near-earth thunderstorms electric field at YBJ (located at YangBaJing, Tibet, China, 4300 m a. s. l.). The variations of the secondary cosmic ray intensity are found to be highly dependent on the strength and polarity of the electric field. In negative fields and in positive fields greater than 600 V/cm, the total number of ground comic ray positrons and electrons increases with increasing electric field strength. And these values increase more obviously when involving a shower with lower primary energy or a higher zenith angle. While in positive fields ranging from 0 to 600 V/cm, the total number of ground comic ray positrons and electrons declines and the amplitude is up to 3.1% for vertical showers. A decrease of intensity occurs in inclined showers within the range of 0−500 V/cm, which is accompanied by smaller amplitudes. In this paper, the intensity changes are analyzed, especially concerning those decreasing phenomena in positive electric fields. Our simulation results could be helpful in understanding the decreases observed in some ground-based experiments (such as the Carpet air shower array and ARGO-YBJ), and also be useful in understanding the acceleration mechanisms of secondary charged particles caused by an atmospheric electric field.

1. Introduction

The effect of thunderstorms electric field on the development of cosmic ray air showers, especially on the intensity of secondary cosmic rays, is one of the hottest topics in high-energy atmospheric physics. During thunderstorms, the maximum strength of electric fields has been found in the range of 850−1300 V/cm [1], or even up to 2000 V/cm [2,3]. In such strong fields, by accelerating or decelerating the charged particles in extensive air showers, the intensity of secondary cosmic rays could be influenced. It was first suggested by Wilson [4] in 1924 that the strong electric field during thunderstorms might result in an observable effect on a secondary electron, which has tiny mass. In 1992, Gurevich et al. [5] suggested an avalanche-type increase of the number of runaway electrons could lead to a new type of electric breakdown of gases in the atmosphere. They developed the theory of runaway breakdown (RB), now mostly referred to as relativistic runaway electron avalanche (RREA) [6]. Marshall et al. [3,7], Dwyer [8] and Symbalisty et al. [9] studied the strength of threshold field necessary for an avalanche to occur, which is strongly dependent on the altitude.

For decades, many scientists have carried out a wide range of ground-based experiments to detect the thunderstorm ground enhancement (TGE), a new high-energy phenomenon originating in the terrestrial atmosphere, trying to find high-energy electrons accelerated by thunderstorms electric field or high-energy photons radiated by bremsstrahlung. The intensity enhancements of ground cosmic rays have been detected by high altitude experiments, such as the Carpet air shower array [10,11], EAS-TOP [12], ASEC [13–17] and ASγ [18]. Their results indicated that the increases were associated with the electric field and the RREA process could be responsible for huge TGEs. Tsuchiya et al. [18–20] and Torii et al. [21–22] provided clear evidence that strong electric fields can accelerate electrons beyond a few tens of MeV.

It is well known that the strong electric discharges associated with thunderstorms can produce terrestrial gamma-ray flash (TGF). For years, thousands of TGFs have been detected by satellite-based experiments, such as AGILE [23] and Fermi-GBM [24]. The lightning initiation and correlations with thunderstorms have also been studied in details [16,25–29].

To discover more valuable information, a few simulations have been done to study the intensity and energy changes of secondary particles during thunderstorms [17,30–32]. Buitink et al. [33] have modified the CORSIKA code and performed simulations to calculate the effect of an electric field on the development of proton showers with energies more than 10^{16} eV. Their results showed that the RREA might occur at high altitudes.

* Corresponding author.
E-mail address: zhouxx@swjtu.edu.cn (X.X. Zhou).

From the experimental observations and simulation results above, it seems that these enhancements of secondary particles during thunderstorms are correlated with the electric field and the RREA will occur under certain conditions. However, the acceleration mechanisms of secondary charged particles caused by atmospheric electric field still remain unresolved.

In 2011, the AGILE team found that the TGF emission above 10 MeV had a significant power-law spectrum with energies up to 100 MeV [34]. These results posed a big challenge for the widely accepted TGF model based on the RREA mechanism.

It is clear now that intensity decreases for the hard component of cosmic rays are associated with thunderstorms electric field. Chilingarian et al. [15] found a deficit of ∼6.0% in the flux of muons with energies greater than 200 MeV during thunderstorms. By analyzing the data from the Carpet air shower array, Alexeenko et al. [11] studied the effects of thunderstorms electric field on the soft and hard components of cosmic rays separately. The net effect is a decreasing intensity for the hard component (muons) and an increasing intensity for the soft component (electrons). Interestingly, a negative correlation of variations between the electric field and the soft component intensity was reported in the same paper. That is to say, the intensity of the soft component decreased in a certain range of positive fields. The study suggested that the reason for this decreasing phenomenon was the poor separation of the soft and hard components. Is the soft component intensity decrease related to thunderstorms electric field or poor separation of the components?

The intensity changes of ground cosmic rays were detected by the ARGO-YBJ experiment, which is connected to two independent data acquisition systems, corresponding to the shower and scaler operation modes. The total counts of charged particles, namely multiplicity (n), are measured every 0.5 s in scaler mode. There are four independent channels to record the counting rates referred to n ≥ 1, 2, 3, 4, respectively. More details about the ARGO-YBJ detector can be found elsewhere [35]. During thunderstorms, the increases for channel n=1 or n=2 are detected. But if n=3 or n ≥ 4, the counting rates do not obviously change or even decline [36–38]. The intensity decreases cannot be explained by the RREA mechanism. Are these decreasing phenomena associated with thunderstorms electric field? Moreover, what is the acceleration mechanism for them?

Because of the unknown strength and structure of thunderstorms electric field, there are numerous problems regarding the processes of high-energy particle interactions in the atmosphere that remain unsolved to this today. In order to learn more about the acceleration mechanism and the intensity change, more theoretical, experimental and careful simulation results are needed.

In this work, we perform Monte Carlo simulations by using CORSIKA to study the effect of a near-earth electric field on the intensity of ground cosmic ray positrons/electrons at YBJ. Using these simulations, we then try to analyze the cause of the decreasing phenomena for soft components. This paper is organized as follows: The simulation parameters are introduced in Section 2. The simulation results of vertical and inclined proton showers with several different primary energies are shown in Section 3. The discussions are presented in Section 4. The conclusions are given in Section 5.

2. Simulation parameters

CORSIKA (COsmic Ray SImulations for KAscade) is a detailed Monte Carlo program used to study the evolution and properties of extensive air showers in the atmosphere [39]. In our simulation work, we use the code of CORSIKA 7.3700, its subroutine ELECTR has been extended to account for the effect of atmospheric electric fields on the transport of electromagnetic particles. The ex-

tension follows the programming procedure emf_macros.mortran, which was developed by Bielajew [40]. The selected hadronic interaction model is QGSJETII-04 for high energy and GHEISHA for low energy.

Previous studies have shown that the atmospheric electric field distributed roughly within the altitude scope of 4−12 km during thunderstorms [41]. Because charged secondary particles will lose their energies quickly through radiation and ionization, the effect on the intensity of charged particles can be neglected in the electric field, which is far from detectors. More details can be found elsewhere [42]. In our simulations, the electric field length is 2000 m, from an altitude of 6300–4300 m (corresponding to the atmospheric depth 484–606 g/cm^2). From the data detected by two electric field mills (Boltek EFM-100) which are installed on the roof of ARGO-YBJ building, we found that the strength of near-earth thunderstorms electric field at YBJ is mostly within 1000 V/cm [43]. In our work, the uniform electric field ranges from –1000 to 1000 V/cm. Here, we define the positive electric field as one that accelerates positrons downward in the direction of the earth.

According to the energy threshold of the ARGO-YBJ detector, which is a few tens of GeV in scaler mode and a few hundreds of GeV in shower mode [35], proton showers with three typical energies of 30, 100 and 770 GeV are chosen as the primary particles in this work.

Since positrons and electrons predominate in the secondary charged particles of cosmic rays, and the hadronic and muonic parts of the shower are hardly affected, the effects of the electric field on positrons and electrons are properly taken into account in our work. In view of the acceleration of the field, the energy cutoff is set to 0.1 MeV, below which value positrons and electrons are discarded from the simulation.

To minimize the fluctuations from shower to shower, we use the same line just like the paper [33]. The differences derived from the first interactions are predominated for extensive air showers. INTTEST option in CORSIKA was selected to simulate the first interaction. All secondary particles after the first interactions were listed in a file, which can be used as an input stack for CORSIKA using the STACKIN option. In this work, we use INTTEST option to make ten thousand shower simulations for vertical and inclined showers with primary energy 30, 100 and 770 GeV. The shower with a large number of secondary particles in the first interaction and a fairly typical longitudinal shower profile was selected. Then we use the selected shower as the input of STACKIN option to generate 2×10^6 showers with different random seeds. This will produce much smaller variations.

3. Simulation results

When a primary cosmic ray enters the atmosphere, it will produce a large number of secondary particles via the hadron and electromagnetic cascades. These particles are distributed in a range many kilometers wide. This phenomenon is called extensive air shower (EAS). The total number of secondary particles, which are produced in an EAS at a particular level in the atmosphere, is called the shower size. In this paper, we only consider the effect of an electric field on positrons and electrons. The shower size is defined as the total number of positrons and electrons.

3.1. Vertical showers with primary energy 100 GeV

The electric fields are chosen as a series of values in the range of –1000−1000 V/cm. The correlations between the number of positrons/electrons and the near-earth electric field are simulated. Fig. 1 shows the percent change of the average number of
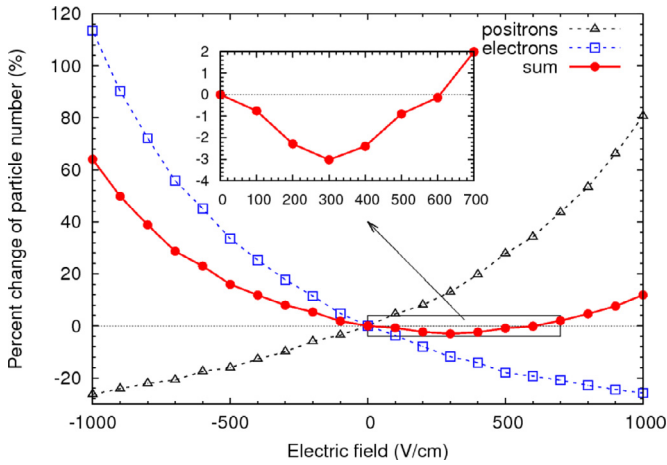
Fig. 1. Percent change of the average number of positrons, electrons and sum of both as a function of electric field at YBJ (The illustration is the enlarged view of the total number in reducing range).
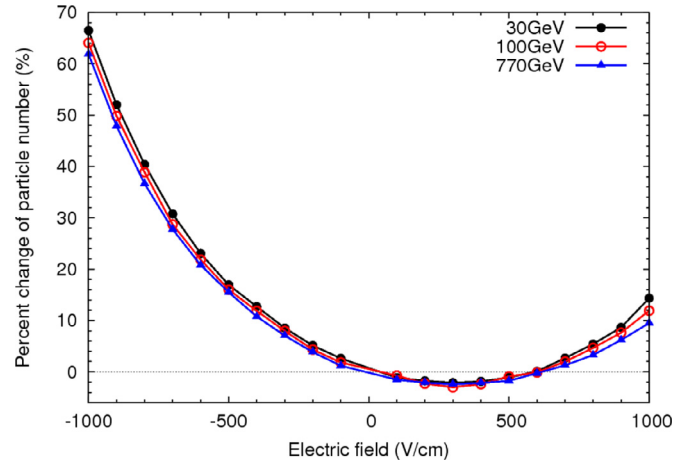

Fig. 2. Percent change of the total number of positrons and electrons as a function of atmospheric depth in 400, 600 and 700 V/cm.

Fig. 3. Percent change of the total number of positrons and electrons as a function of electric field for primary energies of 30, 100 and 770 GeV at YBJ.
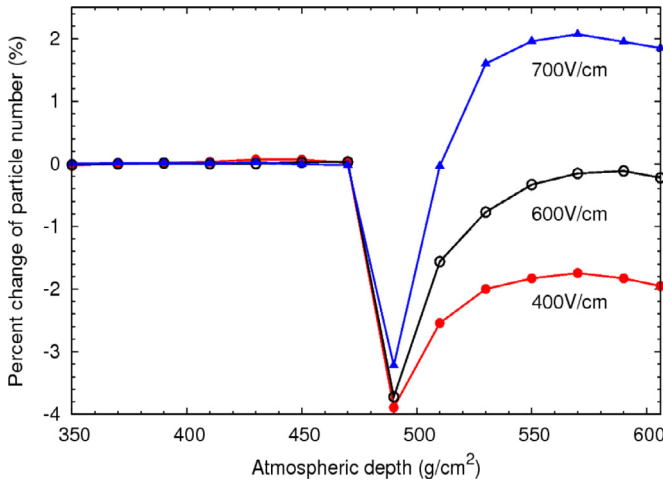
positrons, electrons and the sum of both in different electric fields at YBJ.

As shown in Fig. 1, when the electric field is negative (accelerating electrons), the number of electrons (N_{e-}) increases, while the number of positrons (N_{e+}) decreases. The shower size (total number of positrons and electrons) increases as the electric field strength increases, and the amplitude enhancement is up to 66.5% in an electric field of –1000 V/cm. When the field is positive (accelerating positrons), the number of electrons decreases, while the number of positrons increases. In positive fields greater than 600 V/cm, the shower size increases as the field strength increases, and the amplitude is lower than 14.3% in an electric field of 1000 V/cm. The amplitude of the enhancement is much lower than that in a negative field of the same strength. In the range of 0−600 V/cm, the shower size declines and the maximum amplitude is about 3.1%. From Fig. 1, for proton showers with primary energy 100 GeV, the shower size is enlarged in all negative fields and positive fields greater than 600 V/cm; while in positive fields less than 600 V/cm, the shower size is reduced. That is to say, within the range of 0−600 V/cm, the number of lower shower size is increased and the number of larger shower size is decreased, which results in the decrease of the average shower size.

Fig. 2 shows the percent change of the average shower size as a function of atmospheric depth in several positive electric fields. When the field is switched on from an altitude of 6300 m ($\sim$484 g/cm^2) to 4300 m ($\sim$606 g/cm^2), the shower size drops steeply and the degree of decline reaches up to 3.9%, which is mostly due to more low energy electrons losing their energies to be below the detection threshold in positive fields. Soon, it increases with an increasing atmospheric depth. At YBJ, the shower size is increased in 700 V/cm. While the shower size does not show any significant change in 600 V/cm, it is obviously decreased in 400 V/cm.

3.2. Vertical showers with primary energies of 30, 100 and 770 GeV

This work simulated vertical proton showers with primary energies of 30, 100 and 770 GeV. In Fig. 3, the percent change of the average shower size is plotted as a function of electric field for several shower energies at YBJ. The black solid circle data points correspond to a primary energy of 30 GeV, the red hollow circle points for 100 GeV and the blue solid triangle points for 770 GeV.

As we can see from Fig. 3, in negative fields or in positive fields greater than 600 V/cm, the intensities increase and the amplitude enhancements are larger for showers with lower primary energies. In the 0−600 V/cm range, apparent declines of the total number can be seen for all these different primary energy showers. The differences of the amplitude changes for 30, 100 and 770 GeV are not obvious.

3.3. Inclined showers with primary energy 100 GeV

Fig. 4 shows the results of inclined (with zenith angles of 30 and 60°) proton showers with a primary energy of 100 GeV in different fields at YBJ. The red hollow circle points correspond to showers with a 30° angle and the blue solid triangle points for 60°. Here, vertical showers (black solid circle points) are plotted for reference. As shown in the figure, decreasing phenomena occur in positive fields less than 500 V/cm and the maximum amplitude is about 1.7%, which is smaller than that of the vertical showers. In negative fields and in positive fields greater than 500 V/cm, intensities increase with an increasing field strength and zenith angle. We can see that the effects of positive/negative fields on positrons/electrons of inclined showers are stronger, especially for those with a 60° angle. For other results (such as the longitudinal development) concerning inclined showers, please refer to the report by Buitink et al. [33].
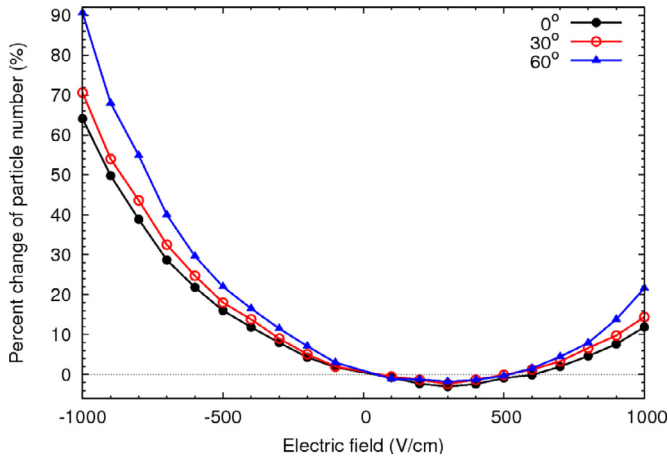
Fig. 4. Percent change of the total number of electrons and positrons as a function of electric field for vertical and inclined showers at YBJ.
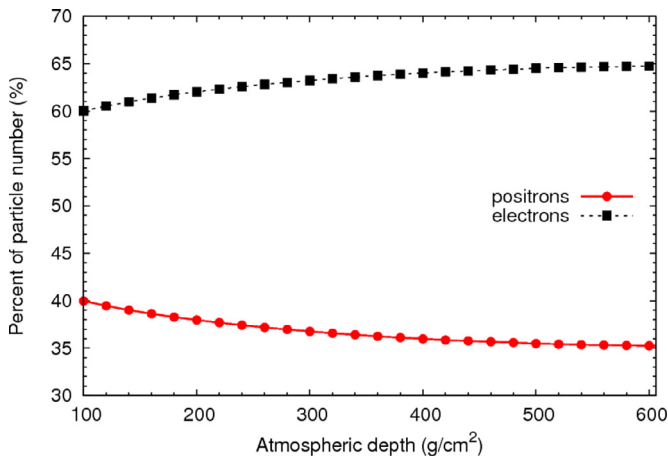

Fig. 6. Ratios of electrons to positrons as a function of electric field at YBJ.

Fig. 5. Percent of electrons and positrons in the total number as a function of atmospheric depth in $E = 0$.

Fig. 7. Percent distributions of electrons and positrons as a function of energy at 6300 m.

3.4. Positrons/electrons distributions for different showers

From our simulation results, we can see that intensity changes of ground cosmic ray positrons/electrons are associated with near-earth thunderstorms electric fields. The degree of intensity increase or decrease is dependent on the polarity and strength of the particular electric field, as well as the primary energy and zenith angle of the shower. We will analyze the electric field effects on the intensity changes especially on the decreasing phenomena as follows: the ratio of electrons to positrons, the energy of positrons and electrons, and the energy and the zenith angle of the primary shower. In the following analyses, if not otherwise specified, all results are for vertical showers with a primary energy of 100 GeV.

3.4.1. The ratio of electrons to positrons

It is well known that the number of positrons is less than that of electrons in cosmic rays for the asymmetry of mechanism, including Compton scattering, positron annihilation and photoelectric effects. Fig. 5 shows the percent of positrons and electrons in the total number as a function of atmospheric depth in absence of an electric field. From our simulation results, we can clearly see that the percentage of positrons decreases as the atmospheric depth increases, while it increases for electrons. For example, at 100 g/cm^2, the number of electrons is about 1.5 times of that of positrons; at YBJ (606 g/cm^2), the value is up to more than
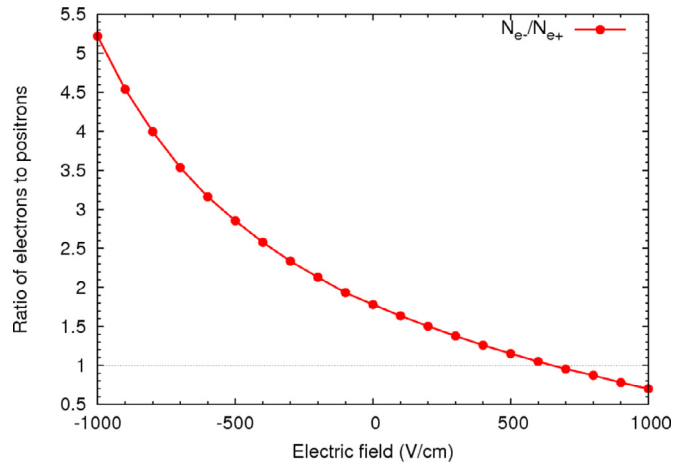
1.8. The reason is mostly that the Compton scattering and photoelectric effects will increase as the atmospheric depth increases.

Fig. 6 shows ratios of electrons to positrons (N_{e^-}/N_{e^+}) in different electric fields at YBJ. In negative fields, the number of electrons is much greater than that of positrons, the ratio is more than 1.8 and the value increases with increasing field strength. In positive fields, positrons are accelerated and low energy positrons gain sufficient energy to be above the detection threshold, and the ratio declines as the field strength increases. In positive fields greater than 600 V/cm, the ratio is less than 1.0 ($<$ 0.75 in 1000 V/cm), which means that positrons outnumber electrons. But in positive fields less than 600 V/cm, the ratio is larger than 1.0, which means that the number of positrons is still less than that of electrons. The number of electrons decreases faster than the number of positrons increase in these fields. This factor ultimately leads to a deficit in total number of positrons and electrons in positive fields less than 600 V/cm.

3.4.2. The energy of positrons and electrons

Fig. 7 shows energy distributions of positrons and electrons at 6300 m in absence of an electric field. In low energy regions, between 1−12 MeV, the proportion of electrons, which is the ratio of electrons in a certain energy region to the total number of electrons, is much larger than that of positrons. But the situation is reversed in higher energy regions. Positrons with energies above 12 MeV become more dominant than that of electrons. For example,
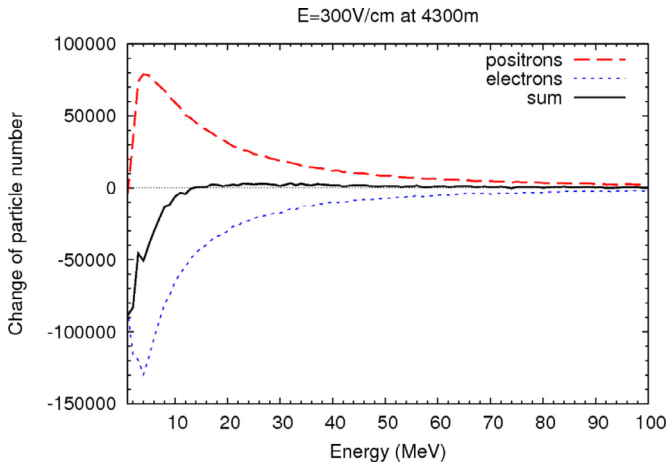
Fig. 8. Number changes of electrons, positrons and sum of both as a function of energy at YBJ in 300 V/cm.

Fig. 9. Percent distributions of positrons and electrons as a function of energy at YBJ in 300 and 1000 V/cm, respectively.

there are 71.7% positrons but only 51.7% electrons with energies more than 12 MeV.

It is well known that the slowing-down force of positron/electron in the atmosphere varies with its energy. According to the theory of Bethe [44], if the energy of positron/electron is more than ∼1 MeV [45], the drag force increases as the energy increases. In electric field, the equilibrium energy (U) [33] of positron/electron can be expressed by $U(X) = \frac{qEZ_0X_0}{X}$, where X is the atmospheric depth with unit g/cm², X0 (∼36.7 g/cm²) is the radiation length for electron/positron in air, Z0 (∼8.4 km) is the scale height, and E is the electric field. Particles below equilibrium energy are accelerated. Radiation losses are dominated for particles above this energy. At the same altitude, the equilibrium energy is higher in stronger fields. For example, at an altitude of 6300 m, the equilibrium energy is about 19.3 MeV in 300 V/cm and 64.2 MeV in 1000 V/cm. From Fig. 7, it can be seen that there are about 59.8% electrons and only 40.9% positrons, which can be accelerated in the field strength of 300 V/cm at 6300 m. It shows that electrons with lower energies are easier to be affected in the same strength field. This factor also leads to a deficit in the total number of positrons and electrons in positive fields.

Fig. 8 shows the number change of positrons, electrons and the sum of both as a function of energy in 300 V/cm at YBJ. When energies are below equilibrium energy, which is less than 19.3 MeV at an altitude lower than 6300 m in 300 V/cm, the number of positrons and electrons changes noticeably. In low energy regions, the increased number of positrons is clearly smaller than the decreased number of electrons. In energies above 12 MeV, the proportions of positrons are larger than that of electrons from Fig. 7, and the total number increases insignificantly. As a result, a decline occurs in 300 V/cm.

Fig. 9 shows the energy distributions of positrons and electrons at YBJ in electric fields of 300 and 1000 V/cm. Solid lines correspond to positrons and dashed lines correspond to electrons. The red thin lines stand for 300 V/cm and blue bold lines stand for 1000 V/cm. As seen in Fig. 9, there are still more positrons with higher energies than that of electrons, and the energies of positrons in 300 V/cm are clearly higher than that in 1000 V/cm. That is to say, more low energy positrons are generated by pair production in 1000 V/cm. Considering the ratio of electrons to positrons and the equilibrium energy, 18.0% of the total particles can be accelerated and 35.4% can be decelerated in 300 V/cm; while in 1000 V/cm, the values vary from 47.5% to 36.6%. It is easy to understand why a decrease occurs in 300 V/cm while an increase occurs in 1000 V/cm.
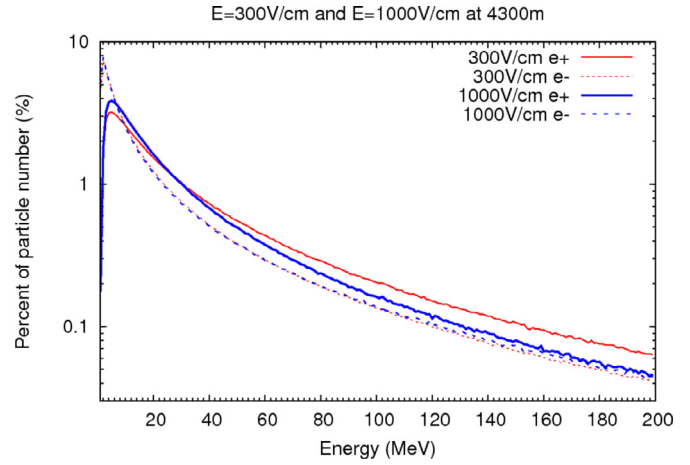
From the analyses above, we know that the number of electrons is greater than that of positrons and there are higher proportions of positrons with larger energies than that of electrons. In certain positive fields, the increase of positrons cannot be compensated by the decrease of electrons, and so an obvious decline in the total number of positrons and electrons occurs.

3.4.3. Primary energy and zenith angle of the shower

In order to understand more about the relations between the intensity changes and the primary energies of showers, we analyze the energy and number distributions of positrons and electrons. Fig. 10(a) shows the energy distributions for showers with 30, 100 and 770 GeV at an altitude of 6300 m. We can see there are more positrons and electrons with larger energies for higher primary energy showers. Fig. 10(b) shows the ratios of electrons to positrons as a function of atmospheric depth in the absence of an electric field. There are more positrons for higher primary energy showers. The reason is mostly that the effect of pair production exceeds the Compton scattering for higher energy showers.

For higher primary energy showers, because of higher energies of positrons/electrons, the effect of the electric field on positrons/electrons is weaker, and the increase in shower size is smaller in negative fields and in positive fields greater than 600 V/cm. In positive fields less than 600 V/cm, the size of the shower with higher primary energy could be easily enlarged for the lower ratio of electrons to positrons, but it is more difficult to accelerate the positrons with higher energies. Because of the contradictory effects of these two factors, the differences of intensity changes are not obvious in the 0–600 V/cm range.

Fig. 11(a) and (b) show the energy distributions and ratios of electrons to positrons for vertical and inclined showers. As for the inclined shower, we only show the results of those with a 60° zenith angle. From the two figures, we can see that the energies and ratios of inclined showers are lower than vertical showers at YBJ. Furthermore, because of the larger atmospheric length for inclined showers, the atmosphere is less dense in the same step length (distance to next interaction). The energy loss due to collisions in low density is smaller and acceleration in the electric field is thus more efficient. The effect of the electric field on the intensity change is stronger for shower with a higher zenith angle.

4. Discussions

During an actual thunderstorm, the strength of electric field fluctuates violently and the polarity can change multiple times. For
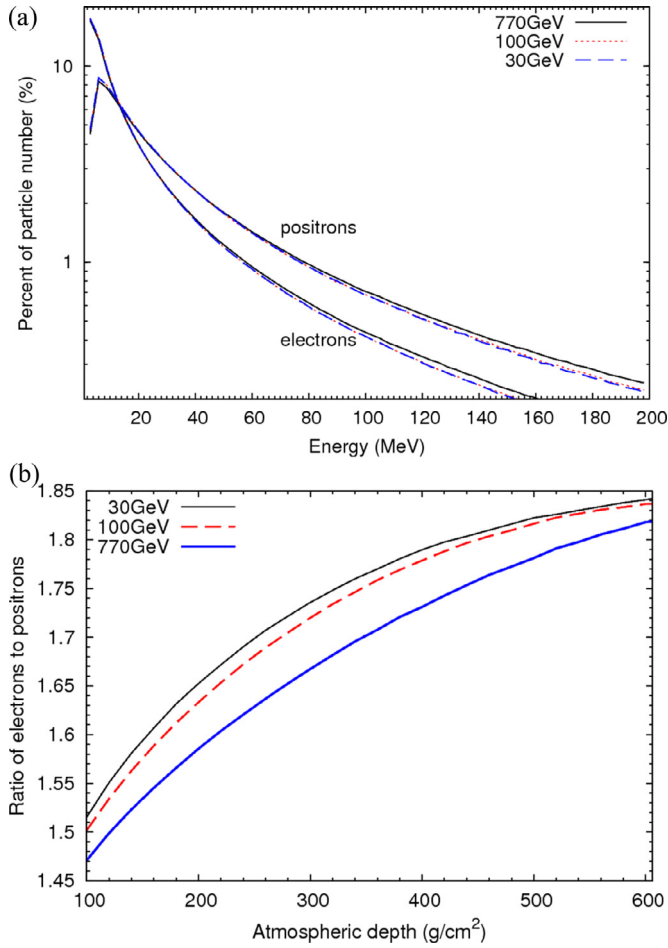
Fig. 10. (top) Percent distributions of electrons and positrons as a function of energy for different primary energies at 6300 m. (bottom) Ratios of electrons to positrons as a function of atmospheric depth for several primary energies in $E=0$.

Fig. 11. (top) Percent distributions of electrons and positrons as a function of energy with zenith angles of 0 and 60° at 6300 m. (bottom) Ratios of electrons to positrons as a function of atmospheric depth with zenith angles of 0 and 60° in $E=0$.

the violent nature, the measurements of the thunderstorm electric fields are difficult to perform. In this work, the electric fields are regarded as homogeneous, which will certainly bring some deviations with the realistic situation. But such simplification could easily clarify the effect of the thunderstorms electric field on the secondary charged particle.

The energy cutoff (0.1 MeV) for positions and electrons is selected for CORSIKA simulation. That means the energy below 0.1 MeV, positions and electrons are discarded before they may be accelerated to higher energies by the electric field. The energy cutoff setting will weaken the effect of the electric field in our simulations.

It has been found by Marshall [7] that the breakeven field strength (E_{BE}) for the energy loss due to collisions is equal to the energy gain in the electric field, which can be expressed by $E_{BE} = E_{th-BE}e^{(-Z/8.4)}$. Dwyer [8] and Symbalisty et al. [9] have studied the threshold field strength (E_{RB}) for the development of a runaway breakdown process, which can be expressed by $E_{RB} = E_{th-RB}e^{(-Z/8.4)}$. Here Z is the height above sea level (the unit is km), E_{th-BE} is about 2020 V/cm at sea level, E_{th-RB} is about 2800 V/cm at sea level. The strength of breakeven field and threshold field are strongly dependent on the altitude. At 6.3 km, E_{BE} is about 950 V/cm and E_{RB} is about 1300 V/cm. According to the RREA mechanism, the breakdown effect occurs when the field strength is higher than threshold field. While the strength is less than breakeven field, no breakdown effects are expected. From Fig. 1, we can see the number of electrons and positrons increases obvi-
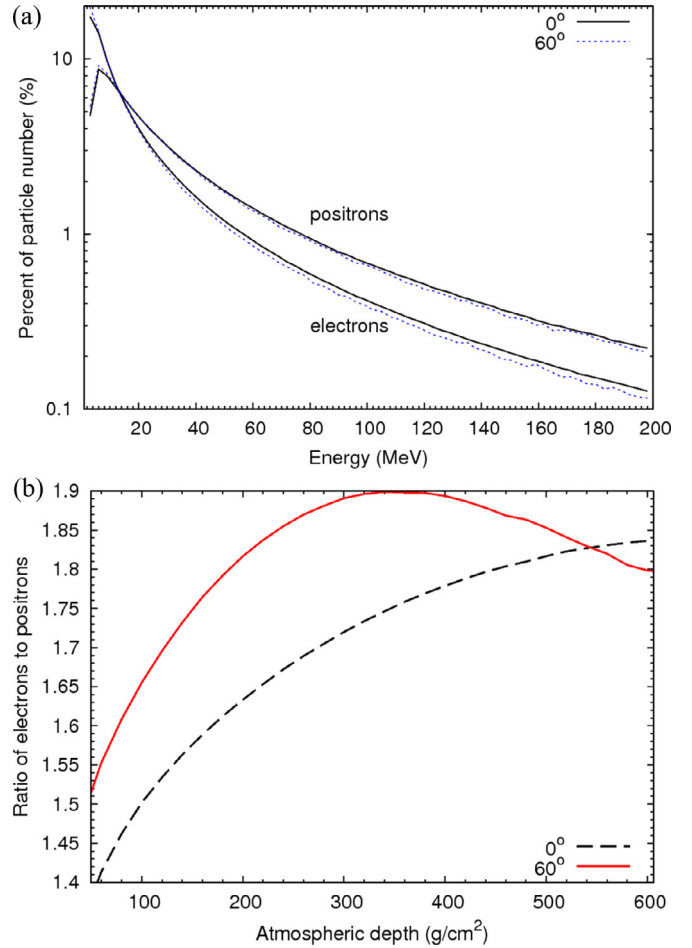
ously when the field is greater than E_{BE}. More detailed discussions of electric field effects about the RREA, please refer to our another paper [43].

Many thunderstorm ground enhancements (TGEs) have been detected by some air shower experiments (such as EAS-TOP, ASEC and ASγ) [12–18]. From our simulation results, these increasing phenomena can be partly explained by the effects of negative fields and a certain range of positive fields on the secondary positrons and electrons.

The decreases of ground cosmic rays have been observed by some high altitude experiments. For soft component, a negative correlation during thunderstorms has been detected by the Carpet air shower array (located at Baksan Valley, North Caucasus, 1700 m a. s. l.) [11]. That is to say, in a certain range of electric fields, an increase in negative fields and a decrease in positive fields occurred. In ARGO-YBJ experiment (located at Tibet, China, 4300 m a. s. l.), an increase of the count rate for channel with lower multiplicity and a decrease for channel with higher multiplicity were observed [36–38]. Comparing with the results obtained from our simulations, there are some similarities, such as the increases or decreases in a certain range of electric fields; while some differences appear, such as the amplitude of the intensity variation and the range of the electric field accompanied with the decline. There are more factors should be taken into account in this simulation, such as the primary energy spectrum, the response of detector, the detection threshold of particle energy and so on. The simulation results in this paper are not able to describe all the observed

phenomenology. But, these results could be helpful in understanding the decreasing phenomena observed in ground-based experiments.

5. Conclusions

Monte Carlo simulations are performed with CORSIKA 7.3700 packages to study the intensity change of ground cosmic rays in near-earth thunderstorms electric fields. We conduct simulations for vertical and inclined (with zenith angles of 30 and 60°) proton showers with primary energies of 30, 100 and 770 GeV. The electric fields are chosen as a series of values in the range of –1000–1000 V/cm, and the length of the fields is 2 km from 6300 m to 4300 m.

The total number of positrons and electrons will increase or decrease in different electric fields. In a negative field, the shower size increases as the field strength increases. The amplitude enhancement is up to 66.5% in –1000 V/cm. In the positive field, the number of positrons continues to increase while the number of electrons continues to decrease. If the positive field is greater than 600 V/cm, the positrons outnumber the electrons at YBJ, and the shower size increases as the field strength increases. The amplitude enhancement is about 14.3% in 1000 V/cm. If the positive field is less than 600 V/cm, the number of electrons remains more than that of positrons. The shower size decreases due to the increase in the number of positrons being less than the decrease in the number of electrons. A certain degree of decline (3.1%) occurs at YBJ in our simulations. The decreases also occur in different primary energy showers and inclined showers. There are two main factors that may be considered for the decreasing phenomenon. First, the number of positrons is less than that of electrons because of the asymmetry of mechanism. Secondly, the electric field has more obvious effects on electrons which have smaller energies than that of positrons.

In 2002, Alexeenko et al. reported that the intensity declines for the soft component of cosmic rays were observed in the Carpet air shower array. During thunderstorms, the decreases of event rates were detected by the ARGO-YBJ experiment. In our simulations, the decreasing phenomena also occur in a certain range of positive fields. Accordingly, we believe the intensity decline of ground cosmic rays, which was detected in mountain top experiments, is really related to the near-earth thunderstorms electric field to some extent. Our simulation results are useful in understanding the observed decreasing phenomenon and give more information about the acceleration mechanism.

References

[1] T.C. Marshall, W.D. Rust, M. Stolzenburg, Electrical structure and updraft speeds in thunderstorms over the southern great plains, J. Geophys. Res. 100 (1995) 1001–1015.
[2] M. Stolzenburg, T.C. Marshall, W.D. Rust, E. Bruning, D.R. MacGorman, T. Hamlin, Electric field values observed near lightning flash initiations, Geophys. Res. Lett. 34 (2007) L04804, doi:10.1029/2006GL028777.
[3] T.C. Marshall, M. Stolzenburg, C.R. Maggio, L.M. Coleman, Observed electric fields associated with lightning initiation, Geophys. Res. Lett. 32 (2005) L03813, doi:10.1029/2004GL021802.
[4] C.T.R. Wilson, The electric field of a thundercloud and some of its effects, Proc. Phys. Soc. 37 (1924) 32D–37D London,.
[5] A.V. Gurevich, G.M. Milikh, R. Roussel-Dupre, Runaway electron mechanism of air breakdown and preconditioning during a thunderstorm, Phys. Lett. A 165 (1992) 463–468, doi:10.1016/0375-9601(92)90348-P.
[6] L.P. Babich, I.M. Kutsyk, E.N. Donskoy, A.Y. Kudryavtsev, New data on space and time scales of relativistic runaway electron avalanche for thunderstorm environment: Monte Carlo calculations, Phys. Lett. A 245 (1998) 460–470, doi:10.1016/S0375-9601(98)00268-0.
[7] T.C. Marshall, W. Rison, W.D. Rust, M. Stolzenburg, J.C. Willett, W.P. Winn, Rocket and balloon observations of electric field in two thunderstorms, J. Geophys. Res. 100 (1995) 20815–20828, doi:10.1029/95JD01877.
[8] J.R. Dwyer, A fundamental limit on electric fields in air, Geophys. Res. Lett. 30 (2003) 2055, doi:10.1029/2003GL017781.
[9] E.M.D. Symbalisty, R. Roussel-Dupre, V.A. Yukhimuk, Finite volume solution of the relativistic Boltzmann equation for electron avalanche studies, IEEE Trans. Plasma Sci. 26 (1998) 1575–1582, doi:10.1109/27.736065.
[10] V.V. Alexeyenko, A.E. Chudakov, V.G. Sborshikov, V.A. Tizengauzen, Short perturbations of cosmic ray intensity and electric field in atmosphere, in: Proceedings 19th ICRC, La Jolla, USA, August 11-23, 5, 1985, pp. 352–355.
[11] V.V. Alexeenko, N.S. Khaerdinov, A.S. Lidvansky, V.B. Petkov, Transient variations of secondary cosmic rays due to atmospheric electric field and evidence for pre-lightning particle acceleration, Phys. Lett. A 301 (2002) 299–306, doi:10.1016/S0375-9601(02)00981-7.
[12] S. Vernetto for EAS-TOP Collaboration, The EAS counting rate during thunderstorms, in: Proceedings of 27th ICRC, Copernicus Gesellschaft, Hamburg, Germany, August 7-15, 10, 2001, pp. 4165–4168.
[13] A. Chilingarian, A. Daryan, K. Arakelyan, Ground-based observations of thunderstorm correlated fluxes of high-energy electrons, gamma rays, and neutrons, Phys. Rev. D 82 (2010) 043009, doi:10.1103/PhysRevD.82.043009.
[14] A. Chilingarian, G. Hovsepyan, A. Hovhannisyan, Particle bursts from thunderclouds: natural particle accelerators above our heads, Phys. Rev. D 83 (2011) 062001, doi:10.1103/PhysRevD.83.062001.
[15] A. Chilingarian, N. Bostanjyan, L. Vanyan, Neutron bursts associated with thunderstorms, Phys. Rev. D 85 (2012) 085017, doi:10.1103/PhysRevD.85.085017.
[16] A. Chilingarian, Thunderstorm ground enhancements-model and relation to lighting flashes, J. Atmosph. Solar-Terrestrial Phys. 107 (2014) 68–76, doi:10.1016/j.jastp.2013.11.004.
[17] A. Chilingarian, B. Mailyan, L. Vanyan, Recovering of the energy spectra of electrons and gamma rays coming from the thunderclouds, Atmos. Res. 114-115 (2012) 1–16, doi:10.1016/j.atmosres.2012.05.008.
[18] H. Tsuchiya, K. Hibino, K. Kawata, et al., Observation of thundercloud-related gamma rays and neutrons in Tibet, Phys. Rev. D 85 (2012) 092006, doi:10.1103/PhysRevD.85.092006.
[19] H. Tsuchiya, T. Enoto, S. Yamada, et al., Detection of high-energy gamma rays from winter thunderclouds, Phys. Rev. Lett. 99 (2007) 165002, doi:10.1103/PhysRevLett.99.165002.
[20] H. Tsuchiya, T. Enoto, T. Torii, Observation of an energetic radiation burst from mountain-top thunderclouds, Phys. Rev. Lett. 102 (2009) 255003, doi:10.1103/PhysRevLett.102.255003.
[21] T. Torii, M. Takeishi, T. Hosono, Observation of gamma-ray dose increase associated with winter thunderstorm and lightning activity, J. Geophys. Res. 107 (2002) 4324–4332, doi:10.1029/2001JD000938.
[22] T. Torii, T. Sugita, S. Tanabe, Y. Kimura, M. Kamogawa, K. Yajima, H. Yasuda, Gradual increase of energetic radiation associated with thunderstorm activity at the top of Mt. Fuji, Geophys. Res. Lett. 36 (2009) L13804, doi:10.1029/2008GL037105.
[23] F. Fuschino, M. Marisaldi, C. Labanti, et al., High spatial resolution correlation of AGILE TGFs and global lightning activity above the equatorial belt, Geophys. Res. Lett. 38 (2011) L14806, doi:10.1029/2011GL047817.
[24] M.S. Briggs, G.J. Fishman, V. Connaughton, et al., First results on terrestrial gamma ray flashes from the fermi gamma-ray burst monitor, J. Geophys. Res. 115 (2010) A07323, doi:10.1029/2009JA015242.
[25] J.R. Dwyer, M.A. Uman, The physics of lightning, Physics Reports 534 (2014) 147–241, doi:10.1016/j.physrep.2013.09.004.
[26] P. Schellart, T.N.G. Trinh, S. Buitink, et al., Probing atmospheric electric fields in thunderstorms through radio emission from cosmic-ray-induced air showers, Phys. Rev. Lett. 114 (2015) 165001, doi:10.1103/PhysRevLett.114.165001.
[27] A. Dubinova, C. Rutjes, U. Ebert, S. Buitink, O. Scholten, G.T.N. Trinh, Prediction of lightning inception by large ice particles and extensive air showers, Phys. Rev. Lett. 115 (2015) 015002, doi:10.1103/PhysRevLett.115.015002.
[28] A.V. Gurevich, A.N. Karashtin, Runaway breakdown and hydrometeors in lightning initiation, Phys. Rev. Lett. 110 (2013) 185005, doi:10.1103/PhysRevLett.110.185005.
[29] A. Chilingarian, G. Hovsepyan, G. Khanikyanc, A. Reymers, S. Soghomonyan, Lighting origination and thunderstorm ground enhancements terminated by the lightning flash, EPL 110 (2015) 49001, doi:10.1209/0295-5075/110/49001.
[30] E.S. Cramer, J.R. Dwyer, S. Arabshahi, I.B. Vodopiyanov, N. Liu, H.K. Rassoul, An analytical approach for calculating energy spectra of relativistic runaway electron avalanches in air, J. Geophys. Res. Space Physics 119 (2014) 7794–7823, doi:10.1002/2014JA020265.
[31] J.R. Dwyer, Implications of x-ray emission from lightning, Geophys. Res. Lett. 31 (2004) L12102, doi:10.1029/2004GL019795.
[32] L.P. Babich, E.I. Bochkov, E.N. Donskoi, I.M. Kutsyk, Source of prolonged bursts of high-energy gamma rays detected in thunderstorm atmosphere in Japan at the coastal area of the Sea of Japan and on high mountaintop, J. Geophys. Res. 115 (2010) A09317, doi:10.1029/2009JA015017.
[33] S. Buitink, T. Huege, H. Falcke, D. Heck, J. Kuijpers, Monte Carlo simulations of air showers in atmospheric electric fields, Astropart. Phys. 33 (2010) 1–12, doi:10.1016/j.astropartphys.2009.10.006.

[34] M. Tavani, M. Marisaldi, C. Labanti, et al., Terrestrial gamma-ray flashes as powerful particle accelerators, Phys. Rev. Lett. 106 (2011) 018501, doi:10.1103/PhysRevLett.106.018501.

[35] G. Aielli for ARGO-YBJ Collaboration, Search For gamma ray bursts with the ARGO-YBJ detector in scaler mode, Astrophys. J. 699 (2009) 1281–1287, doi:10.1088/0004-637X/699/2/1281.

[36] X.M. Zhou, N. Ye, F.R. Zhu, et al., Observing the effect of the atmospheric electric field inside thunderstorms on the EAS with the ARGO-YBJ experiment, in: Proceedings of *32nd ICRC*, Beijing, China, August 11-18, 11, 2011, pp. 287–290.

[37] B. Xu, Y.G. Bie, D. Zou, Study of the instantaneous change of secondary cosmic ray during thunderstorm, Chin. J. Space Sci. 32 (2012) 501–505.

[38] Y. Zeng, F.R. Zhu, H.Y. Jia, et al., Correlation between cosmic ray flux and electric atmospheric field variations with the ARGO-YBJ experiment, in: Proceedings of *33rd ICRC*, Rio de Janeiro, Brazil, July 2-9, 2013, pp. 0757–0760.

[39] D. Heck, J. Knapp, et al., CORSIKA: A Monte Carlo Code to Simulate Extensive Air Showers, FZKA: Forschungszentrum Karlsruhe GmbH, Karlsruhe, 6019, 1998 Available from http://www-ik.fzk.de/corsika/physics_description/corsika_phys.html.

[40] A.F. Bielajew, in: *Electron Transport in **E** and **B** Fields, in Monte Carlo Transport of Electrons and Photons*, Plenum Press, New York, 1988, pp. 421–434.

[41] D.X. Liu, X.S. Qie, Z.C. Wang, X.K. Wu, L.X. Pan, Characteristics of lightning radiation source distribution and charge structure of squall line, Acta Phys. Sin. 62 (2013) 219201, doi:10.7498/aps.62.219201.

[42] X.X. Zhou, X.J. Wang, D.H. Huang, H.Y. Jia, Effects of thunderstorms electric field on intensity of cosmic ray electrons, Chin. J. Space Sci. 36 (2016) 49–55, doi:10.11728/cjss2016.01.049.

[43] X.X. Zhou, X.J. Wang, D.H. Huang, H.Y. Jia, C.Y. Wu, Simulation study on the correlation between the ground cosmic rays and the near earth thunderstorms electric field at Yangbajing (Tibet China), Acta Phys. Sin. 64 (2015) 149202, doi:10.7498/aps.64.149202.

[44] H.A. Bethe, Theory of passage of swift corpuscular rays through matter, Ann. Phys. 5 (1930) 325–400.

[45] R. Roussel-Dupre, A.V. Gurevich, On runaway breakdown and upward propagating discharges, J. Geophys. Res. 101 (1996) 2297–2311, doi:10.1029/95JA03278.